Electronic Supplementary Material (ESI) for ChemComm.

Supporting Information

Enhanced Basicity of an Electron Donor-Acceptor Complex

Bernard G. Stevenson,[a] Amanda V. Prascsak,[b] Annemarie A. Lee, [a] Eric D. Talbott,[a] Lisa A. Fredin*[b] and John R. Swierk*[a]

a. Department of Chemistry, State University of New York at Binghamton, Vestal, NY 13850

b. Department of Chemistry, Lehigh University, 6 E. Packer Ave, Seeley G. Mudd, Bethlehem, PA 18015

Table of Contents

General Methods:

1,4-dicyanobenzene (DCB), tetramethylsilane (TMS) and trifluoroacetic acid were purchased from Millipore Sigma and used as received. 1-phenylpyrrolidine (NPP) was purchased from Fisher Scientific and used as received. Deuterated acetonitrile (acetonitrile-d_3) was purchased from Cambridge Isotope Laboratories and used as received.

^{1}H NMR was recorded on a Bruker Avance III HD 400. The ^{1}H NMR spectrum was calibrated to the acetonitrile-d_3 solvent residual peak at δ1.94.^{1}H NMR are reported as follows: chemical shift (δ ppm), integration, multiplicity (s = singlet, d = doublet, t = triplet, q = quartet, m = multiplet) and coupling constant (Hz).

NMR Characterization:

1-phenylpyrrolidine: ^{1}H NMR (400 MHz, CD_3CN) δ7.17 (t,2H, J=8.31Hz), 6.57 (q, 4H), 3.23 (m, 4H), 1.98 (m, 4H)

1,4-Dicyanobenzene: ^{1}H NMR (400 MHz, CD_3CN) 7.888 (s,4H)

Electron Donor Acceptor Complex Absorption Spectrum

The UV-Vis absorption spectrum of the electron donor-acceptor complex was carried out using a Shimadzu UV-2600. Solutions of 50 mM NPP, 50 mM DCB, and 50 mM DCB/NPP in ACN were made. UV-Vis baselined to the solvent. Using 4-side glass cuvette spectra of each component were taken at 325-800 nm.

NPP and 1,4 DCB NMR Study:

Stock solutions of DCB (0.01 M) and NPP (0.01 M) were prepared in acetonitrile-d_3. About 3 drops of the NMR standard, TMS, was added to the DCB stock solution. 600 µL NMR samples were made with a combination of DCB and NPP, while keeping DCB concentration constant. Each NMR tube was securely capped and inverted to achieve a homogenous sample. The corresponding shifts of the DCB peak were then recorded and calibrated through the TMS peak as the concentrations of NPP were varied.

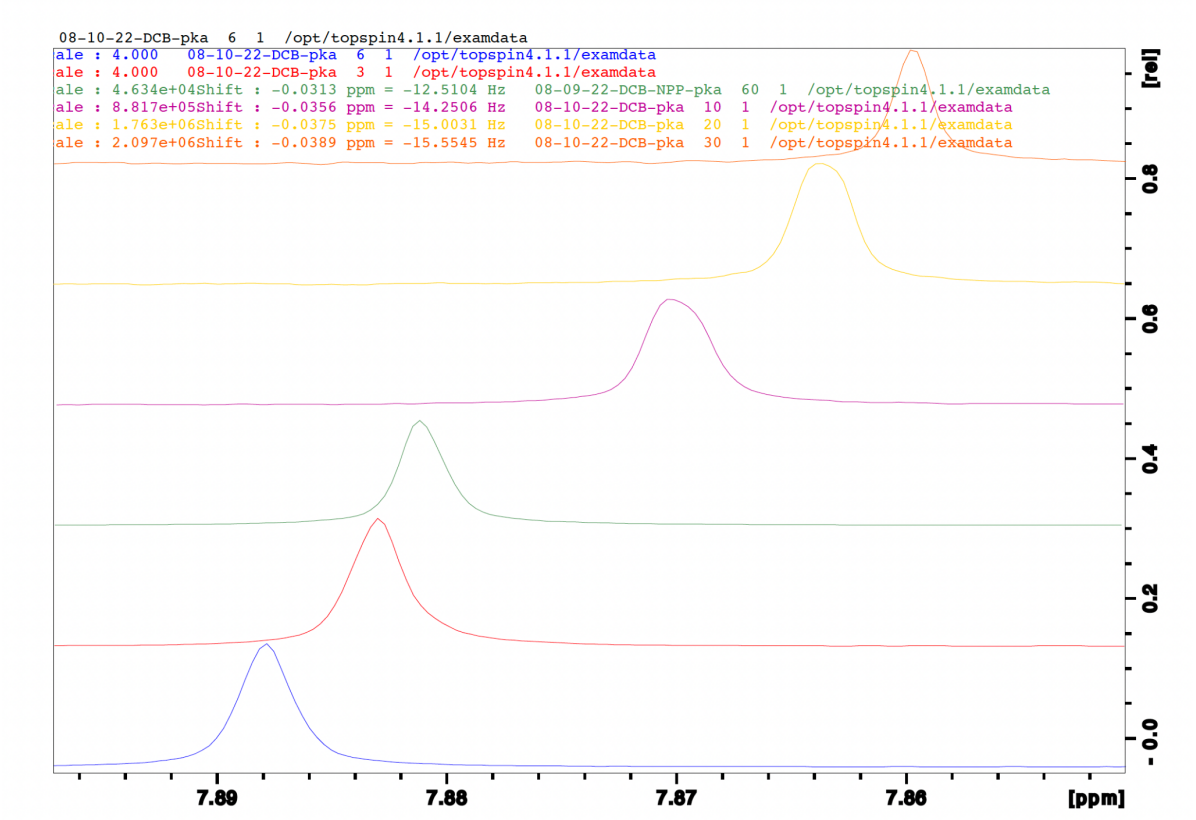

Figure S1. ^{1}H NMR spectra increasing concentration of NPP to DCB. Spectra containing the DCB shifts up-field as the concentration of NPP increases. From bottom to top the equivalents of NPP to DCB are 0, 1, 5, 10, 25 and 50.

Table S1. Concentration and chemical shift data for titration of DCB with NPP.

Concentration of NPP (M)	Change in Shift (ppm)	DCB Chemical Shift (ppm)
0.000034	-0.001475	7.8864
0.000085	-0.002725	7.8851
0.00017	-0.00505	7.8828
0.00034	-0.006275	7.8816
0.000425	-0.011775	7.8761
0.00068	-0.01095	7.8769
0.00085	-0.022725	7.8651
0.00119	-0.01545	7.8724
0.00136	-0.0188	7.8690
0.0017	-0.017375	7.8705
0.00187	-0.0283	7.8595
0.00204	-0.026725	7.8611
0.00221	-0.028625	7.8592
0.00238	-0.028725	7.8591
0.00255	-0.021725	7.8661
0.00289	-0.02915	7.8587
0.00306	-0.022225	7.8656
0.0034	-0.027575	7.8603
0.00357	-0.029475	7.8584
0.00391	-0.029225	7.8586
0.00425	-0.024075	7.8638
0.00459	-0.027825	7.8600
0.00476	-0.0297	7.8581
0.0051	-0.028075	7.8598
0.00595	-0.026175	7.8617
0.0085	-0.028275	7.8596

Computation:

Quantum Chemistry. Structure optimizations were performed in Gaussian16[2] using the hybrid M06-L functional and a triple-ζ basis set with polarization, 6-311g(d,p). An acetonitrile polarization continuum model of solvation was applied to allow for more charge localization, and GD3 empirical dispersion was used to account for the diffuse π-bonds. Harmonic vibrational frequencies were used to estimate zero-point energy (ZPE) and the thermal contributions free energies at 298.15K, as well as to ensure intermediates were minima on the potential energy surface. Basis set superposition errors (BSSE) were calculated for all dimers with no solvent or dispersion as that is not supported in Gaussian16. The dimer Gs = EE + ZPE + Thermal contributions + BSSE.

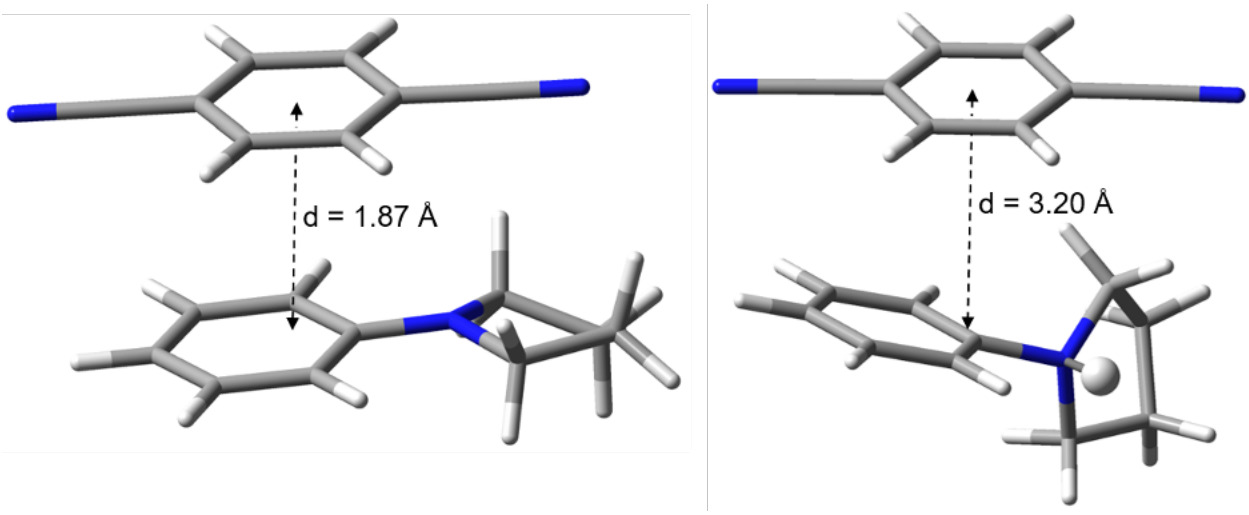

Figure S2. D3-M06-L/6-311g(d,p)/PCM(ACN) optimized EDA dimer and $EDAH^+$.

Table S2. D3-M06-L/6-311g(d,p)/PCM(ACN) Calculated parameters.

	E (Hartrees)	G[a] (Hartrees)
DCB	-416.779	-416.7153
NPP	-443.6855	-442.5111
NPPH+	-444.0531	-442.8654
DCB-NPP	-860.4802	-860.2179
DCB-NPPH+	-860.8386	-860.5628

[a]BSSE corrected for the dimers

Table S3. M06-L/6-311g(d,p) Calculated Energetics.[a]

	ΔG (kcal/mol)
DCB + NPP → DCB-NPP	-5.32
DCB + NPPH+ → DCB-NPPH+	-11.26
NPP → NPPH+	-222.35
DCB-NPP→ DCB-NPPH+	-216.41

[a]These energies provide only relative information on favorability but the need to include BSSE without solvent or dispersion limits their experimental relevance.

Table S4. D3-M06-L/6-311g(d,p)/PCM(ACN) Calculated charges.

	pyrrolidine N Mulliken charge
DCB	-
NPP	-0.511
1-methylpyrrolidine	-0.437
NPPH+	-0.420
DCB-NPP	-0.481
DCB-NPPH+	-0.326
DCB-1-methylpyrrolidine dimer	-0.00149

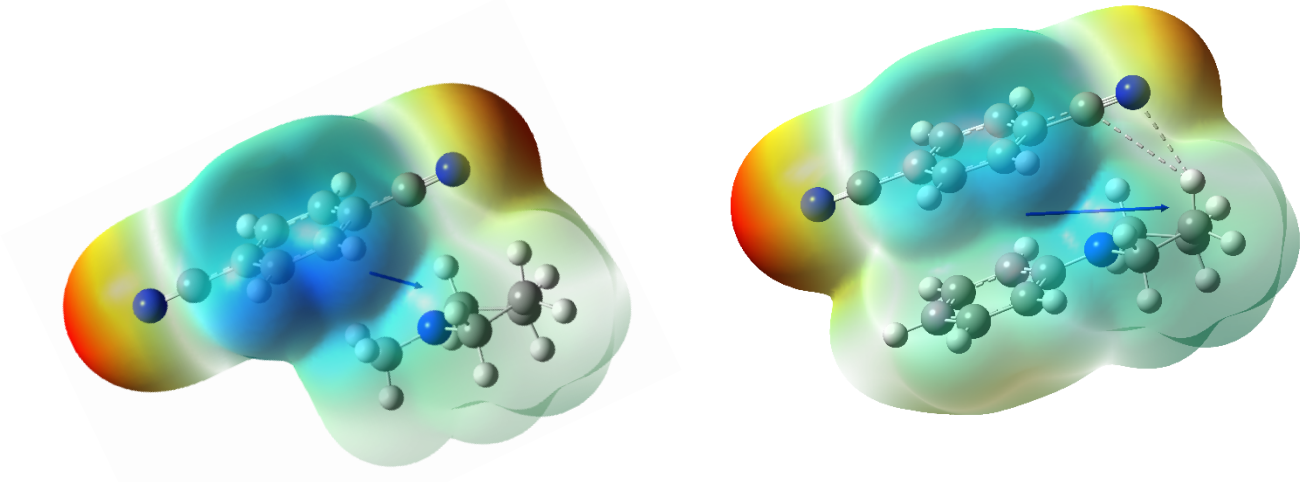

Figure S3. D3-M06-L/6-311g(d,p)/PCM(ACN) charge distributions and dipole moments in the DCB-1-methylpyrrolidine and EDA dimer.

NPP and TFA NMR Study:

Stock solutions of 0.1152 M 1-phenylpyrrolidine (NPP), 0.2304 M trifluoroacetic acid (TFA) and 0.9216 M TFA in acetonitrile-d_3 were prepared. 200 µL of 0.1152 M NPP and corresponding equivalents of TFA were added to an NMR tube. Acetonitrile-d_3 was then added so that the total volume of the NMR tube was 600 µL. The NMR tube was then capped and inverted several times to ensure homogeneity. The ^{1}H NMR spectra were then calibrated and the shift of the NPP peaks at δ3.23 were recorded.

Table S5. Concentration and chemical shift data for titration of NPP with TFA.

Concentration TFA (M)	NPP Chemical Shift Peak (δ)	NPP Chemical shift change ($\Delta\delta$)
0	3.2366	0
0.00384	3.2511	0.0145
0.0192	3.3296	0.093
0.0384	3.4334	0.1968
0.0576	3.5166	0.28
0.0768	3.5958	0.3592
0.096	3.6311	0.3945
0.1152	3.6723	0.4357
0.1344	3.6915	0.4549
0.1536	3.7172	0.4806
0.192	3.7378	0.5012
0.2304	3.7474	0.5108
0.2688	3.7502	0.5136
0.3072	3.7531	0.5165
0.3456	3.7543	0.5177
0.384	3.7556	0.519
0.4224	3.7564	0.5198

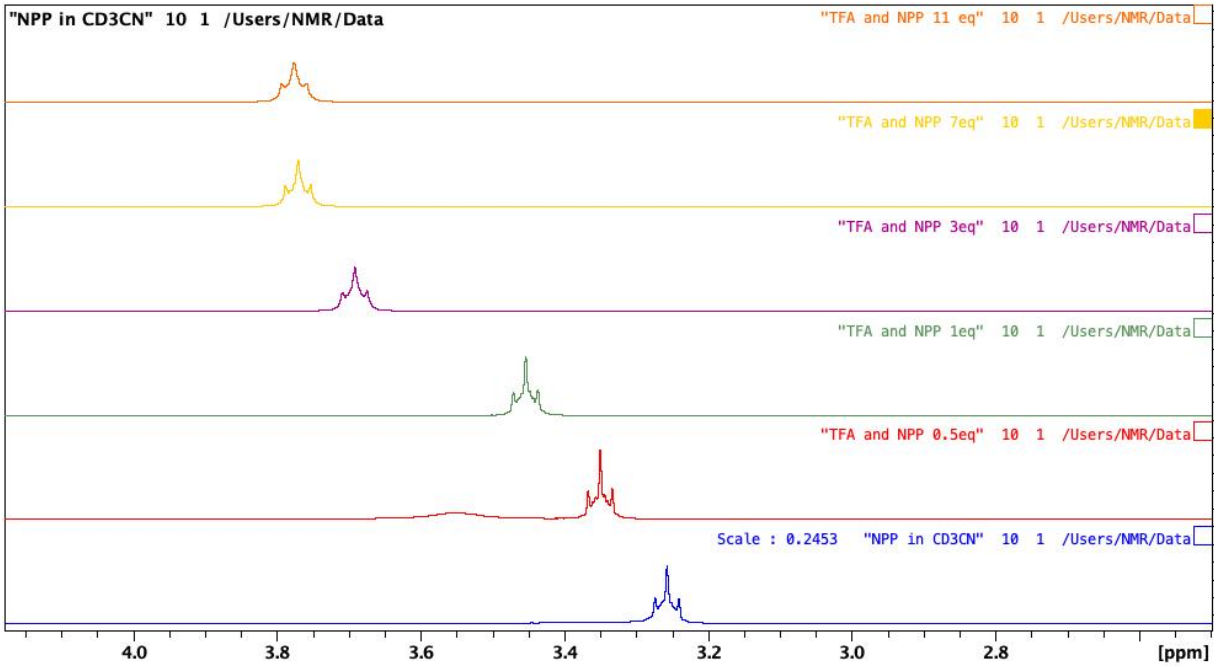

Figure S4. ^{1}H NMR spectra NPP hydrogen shift with increasing concentration of TFA (starting **δ** =3.256). Going from bottom to top the equivalences of TFA to NPP are 0, 0.5, 1,3, 7 and 11. NPP α-amino hydrogen shifts downfield as TFA concentration is increased.

NPP/1,4-DCB and TFA NMR Study:

Stock solutions of DCB (0.150 M) and NPP (0.020) were prepared in acetonitrile-d_3. 2 drops of the NMR standard, TMS, was added to the DCB/NPP EDA complex stock solution. 600 µL NMR samples were made with DCB/NPP stock and TFA. Each NMR tube was securely capped and inverted to achieve a homogenous sample. The corresponding shifts of the EDA NPP peak were then recorded and calibrated through the TMS peak as varying concentrations of TFA were added.

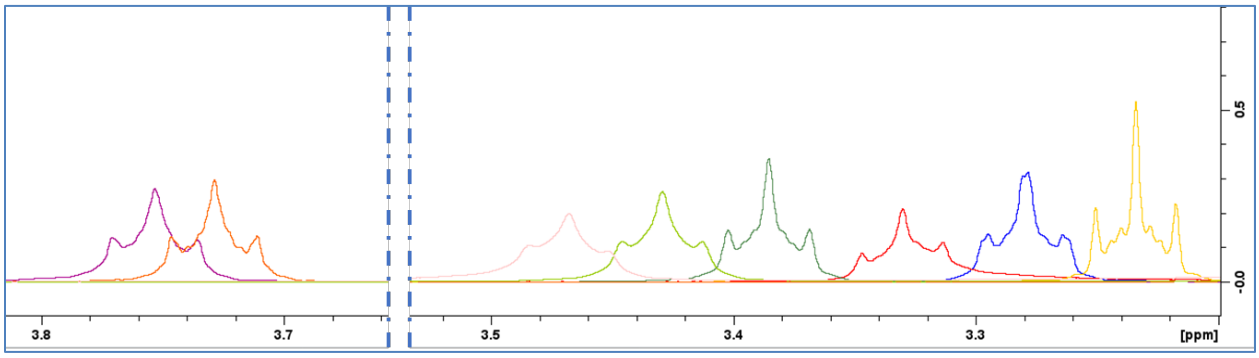

Figure S5. ^{1}H NMR spectra increasing concentration of TFA to DCB/NPP EDA complex. Spectra containing the NPP α-amino hydrogen (starting **δ** =3.234) shift with the increasing concentration of TFA. 1,4-DCB/NP EDA complexed was kept constant at 0.010 M. From right to left the equivalents of TFA are 0, 0.275, 0.55, 0.825, 1.375, 7.32, and 14.6 to the EDA complex. As TFA is increased, the NPP α-amino hydrogen chemical shifts downfield.

Table S6. Concentration and chemical shift data for titration of DCB/NPP EDA complex with TFA.

Conc. of TFA (M)	Chemical Shift (**δ**)	Change in Chemical Shift (Δ**δ**)
0	3.2338	0
2.75E-03	3.2783	0.0445
5.50E-03	3.3301	0.0963
8.25E-03	3.3852	0.1514
1.10E-02	3.4291	0.1953
1.38E-02	3.4679	0.2341
1.65E-02	3.5073	0.2735
1.93E-02	3.5413	0.3075
2.20E-02	3.5687	0.3349
2.48E-02	3.5899	0.3561
2.75E-02	3.6185	0.3847
3.66E-02	3.6607	0.4269
7.32E-02	3.7285	0.4947
1.10E-01	3.73	0.4962
1.46E-01	3.7355	0.5017

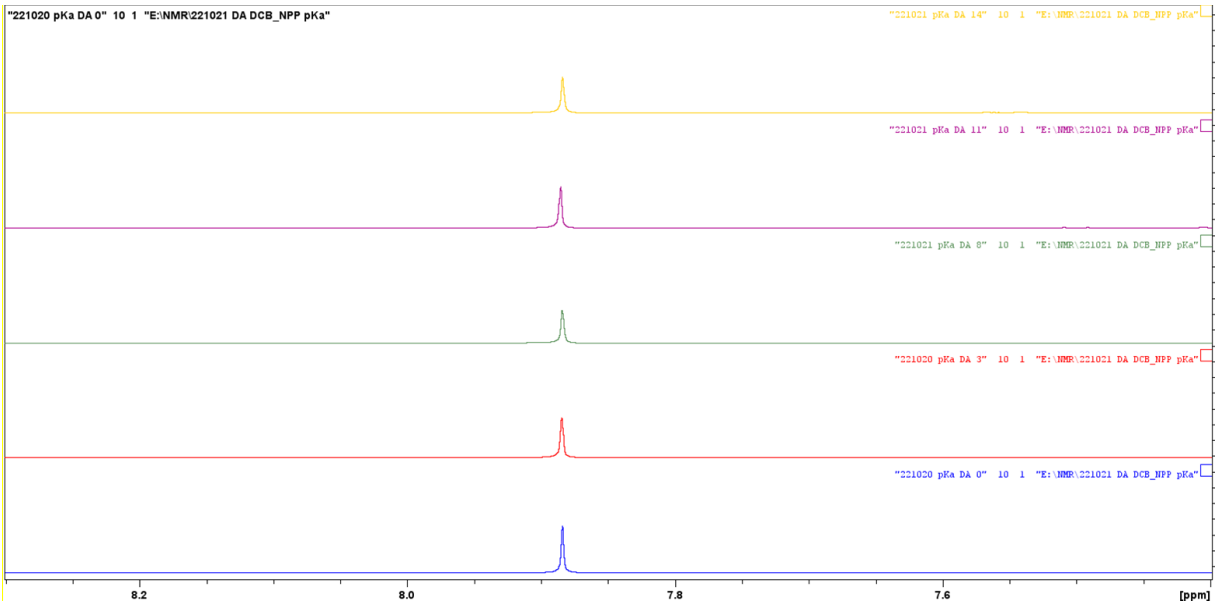

Figure S6. ^{1}H NMR spectra with increasing concentration of TFA to DCB/NPP EDA complex. Spectra shows the DCB singlet shift remaining constant with increased TFA addition. From bottom to top, the TFA molar equivalence to DCB/NPP EDA are 0, 0.825, 2.2, 7.32, and 14.6.

References:

1. F. H. Stootman, D. M. Fisher, A. Rodger, and J. R. Aldrich-Wright, *Analyst*, 2006, **131**, 1145-1151.

2. Gaussian 16, Revision C.01, Frisch, M. J.; Trucks, G. W.; Schlegel, H. B.; Scuseria, G. E.; Robb, M. A.; Cheeseman, J. R.; Scalmani, G.; Barone, V.; Petersson, G. A.; Nakatsuji, H.; Li, X.; Caricato, M.; Marenich, A. V.; Bloino, J.; Janesko, B. G.; Gomperts, R.; Mennucci, B.; Hratchian, H. P.; Ortiz, J. V.; Izmaylov, A. F.; Sonnenberg, J. L.; Williams-Young, D.; Ding, F.; Lipparini, F.; Egidi, F.; Goings, J.; Peng, B.; Petrone, A.; Henderson, T.; Ranasinghe, D.; Zakrzewski, V. G.; Gao, J.; Rega, N.; Zheng, G.; Liang, W.; Hada, M.; Ehara, M.; Toyota, K.; Fukuda, R.; Hasegawa, J.; Ishida, M.; Nakajima, T.; Honda, Y.; Kitao, O.; Nakai, H.; Vreven, T.; Throssell, K.; Montgomery, J. A., Jr.; Peralta, J. E.; Ogliaro, F.; Bearpark, M. J.; Heyd, J. J.; Brothers, E. N.; Kudin, K. N.; Staroverov, V. N.; Keith, T. A.; Kobayashi, R.; Normand, J.; Raghavachari, K.; Rendell, A. P.; Burant, J. C.; Iyengar, S. S.; Tomasi, J.; Cossi, M.; Millam, J. M.; Klene, M.; Adamo, C.; Cammi, R.; Ochterski, J. W.; Martin, R. L.; Morokuma, K.; Farkas, O.; Foresman, J. B.; Fox, D. J. Gaussian, Inc., Wallingford CT, 2016.